Acta Biomaterialia 18 (2015) 68–76

Contents lists available at ScienceDirect

Acta Biomaterialia

journal homepage: www.elsevier.com/locate/actabiomat

Cisplatin-loaded polymeric nanoparticles: Characterization and potential exploitation for the treatment of non-small cell lung carcinoma

Chunshan Shi [a,c,1], Haiyang Yu [b,1], Dejun Sun [a,*], Lili Ma [b], Zhaohui Tang [b,*], Qiusheng Xiao [c], Xuesi Chen [b]

[a] College of Pharmacy, Jilin University, Changchun 130021, Jilin, PR China
[b] Key Laboratory of Polymer Ecomaterials, Changchun Institute of Applied Chemistry, Chinese Academy of Sciences, Changchun 130022, PR China
[c] The People's Liberation Army 208th Hospital 461 Clinical Departments, Changchun 130021, Jilin, PR China

ARTICLE INFO

Article history:
Received 14 October 2014
Received in revised form 13 January 2015
Accepted 12 February 2015
Available online 20 February 2015

Keywords:
NSCLC
Glutamic acid
Cisplatin
Nanoparticle
Metabolism

ABSTRACT

Cisplatin-loaded poly(L-glutamic acid)-*g*-methoxy poly(ethylene glycol 5K) nanoparticles (CDDP-NPs) were characterized and exploited for the treatment of non-small cell lung carcinoma (NSCLC). *In vitro* metabolism experiments showed that a glutamic acid 5-mPEG ester [$CH_3O(CH_2CH_2O)_n$Glu] was generated when the poly(L-glutamic acid)-*g*-methoxy poly(ethylene glycol 5K) (PLG-*g*-mPEG5K) was incubated with HeLa cells. This suggests that the poly(glutamic acid) backbone of the PLG-*g*-mPEG5K is biodegradable. Furthermore, the size of the CDDP-NPs in an aqueous solution was affected by varying the pH (5.0–8.0) and their degradation rate was dependent on temperature. The CDDP-NPs could also bind to the model nucleotide 2′-deoxyguanosine 5′-monophosphate, indicating a biological activity similar to cisplatin. The CDDP-NPs showed a significantly lower peak renal platinum concentration after a single systemic administration when compared to free cisplatin. *In vivo* experiments with a Lewis lung carcinoma (LLC) model showed that the CDDP-NPs suppressed the growth of tumors. In addition, LLC tumor-bearing mice treated with the CDDP-NPs (5 mg/kg cisplatin eq.) showed much longer survival rates (median survival time: 51 days) as compared with mice treated with free cisplatin (median survival time: 18 days), due to the acceptable antitumor efficacy and low systemic toxicity of CDDP-NPs. These results suggest that the CDDP-NPs may be successfully applied to the treatment of NSCLC.

1. Introduction

Currently, lung cancer is one of the most serious diseases threatening people's health in the world [1,2]. Lung cancer can be divided into two main types based on bionomics, therapeutics and prognosis: non-small cell lung cancer (NSCLC) and small cell lung cancer (SCLC) [3]. The former type accounts for 85% of all diagnosed cases of lung cancer, with complex bionomics, more serious malignancy and a higher recurrence rate [4]. Presently, the main clinical therapeutic options include surgery, radiotherapy and chemotherapy combined with biotherapy. Surgery and radiotherapy are considered to be loco-regional tumor treatments. Biotherapy is a new adjuvant therapy that has not yet matured. Thus, chemotherapy is still necessary for the NSCLC patient in either the preoperative or postoperative period.

Platinum-based doublets (platinum plus a new agent) are the standard of care for first-line chemotherapy in the treatment of advanced NSCLC [5,6]. As a typical platinum-based anticancer agent, cisplatin (cis-diaminodichloroplatinum, CDDP) is recommended as the first-line treatment for NSCLC due to its strong anti-cancer effects, synergism with other anti-cancer agents, no cross-resistance and advantages toward response and survival [7]. Cisplatin is toxic to cells due to formation of inter- and intra-strand cross-linked DNA adducts that activate apoptosis [8–10]. Despite the great success in treating NSCLC, cisplatin has several side-effects that limit its use; severe renal toxicity (nephrotoxicity) is often a major concern [11,12]. Recently, cisplatin-induced nephrotoxicity has been significantly reduced through the use of a vigorous hydration regimen that includes prehydrating with isotonic saline and posthydrating with normal saline, mannitol and furosemide [13–15]. However, despite these precautions, cisplatin-induced nephrotoxicity was still reported in 32% of patients observed. Among these patients, 14% developed irreversible renal failure [16]. Cisplatin's nephrotoxicity is attributed to two main factors: high concentrations of cisplatin in the kidneys and adverse impacts on the renal transport system. Cisplatin-induced nephrotoxicity is dose-dependent, and thus limits the possibility of increasing dosages; consequently, treatment effectiveness is

* Corresponding authors.
E-mail addresses: sundejun@163.com (D. Sun), ztang@ciac.ac.cn (Z. Tang).
[1] These authors contributed equally to this work.

http://dx.doi.org/10.1016/j.actbio.2015.02.009
1742-7061/

impaired [11]. Therefore, reducing cisplatin-induced nephrotoxicity is highly desirable for the treatment of NSCLC.

Nanotechnology provides a powerful tool for decreasing the overall concentration of cisplatin in the kidneys along with the concentration ratio of cisplatin between the kidneys and blood [17]. The renal filtration threshold is ~5.5 nm, implying that larger nanoparticles may not significantly accumulate in the kidneys [18]. In addition, the blood circulation of nanoparticles is remarkably prolonged through PEGylation [19–21]. Therefore, PEGylated nanoparticles that are sufficiently large to avoid renal filtration, in particular, have great potential for decreasing the overall concentration of cisplatin in the kidneys as well as the concentration ratio of cisplatin between the kidneys and the blood. As a matter of fact, NC-6004 (cisplatin-incorporated PEG-polyglutamate block copolymer micelles) with a diameter of approximately 30 nm showed a 65-fold area under the curve value and reduced nephrotoxicity in rats as compared with free cisplatin. The peak renal Pt concentration was 3.8-fold lower in animals given NC-6004 than in animals given CDDP [12]. Yu et al. showed that cisplatin-loaded nanoparticles that use a graft copolymer of poly(L-glutamic acid)-*g*-methoxy poly(ethylene glycol) as a carrier had an advantage over those prepared from a PEG-polyglutamate block copolymer for improving blood circulation time [22]. These data indicate that cisplatin-loaded nanoparticles may be suitable for the treatment of NSCLC.

Previously, we reported the influences of the processing procedure and the properties of polymeric carrier materials on plasma pharmacokinetics, biodistribution and *in vivo* efficacy of CDDP-NPs [22]. In the present study, we investigated the *in vitro* metabolism of the poly(L-glutamic acid)-*g*-methoxy poly(ethylene glycol) polymer, the size of cisplatin-loaded PLG-*g*-mPEG nanoparticles at various pH, the degradation of the CDDP-NPs in aqueous solution, the mechanism of action and the renal platinum accumulation of the CDDP-NPs. In addition, we evaluated the cytotoxicity and hemocompatibility of the CDDP-NPs by using an MTT and hemolysis assay. Finally, we investigated the antitumor efficacy and systemic toxicity of the CDDP-NPs compared with free CDDP in mice bearing murine non-small cell lung cancer (Lewis Lung Carcinoma, LLC) tumors.

2. Experimental section

2.1. Materials

LLC and HeLa cell lines were used in the experiments. We cultured the LLC and HeLa cells at 37 °C in a 5% CO_2 atmosphere in Dulbecco's modified Eagle's medium (DMEM, Gibco) supplemented with 10% fetal bovine serum (FBS), penicillin (50 U mL^{-1}) and streptomycin (50 U mL^{-1}). Cisplatin was bought from Shandong Boyuan Chemical Company, China. Poly(L-glutamic acid)-*g*-methoxy poly (ethylene glycol 5K) (PLG-*g*-mPEG5K, Scheme 1) and cisplatin loaded PLG-*g*-mPEG5K complex nanoparticles (CDDP-NPs, 0.50 mg/mL in distilled water on the basis of cisplatin) were prepared by a procedure that is reported elsewhere [22]. In brief, the PLG-*g*-mPEG5K was prepared by an esterification reaction of poly(L-glutamic acid) (M_n = 20.7 × 10^3 g/mol, PDI = 1.36, polyethylene glycol as the standard) with mPEG5K (M_W = 5000 g/mol, Aldrich) in a mass ratio of 1:2. The M_n and PDI (polyethylene glycol as the standard) of the obtained PLG-*g*-mPEG5K were 37.3 × 10^3 g/mol and 1.91, respectively. The CDDP-NPs were prepared by the complexation of PLG-*g*-mPEG5K with CDDP in an aqueous solution at 37 °C for 72 h in the dark with sequential ultrafiltration purification (molecular weight cut-off size: 50 × 10^3 Da) as we previously reported [22]. The CDDP loading content, hydrodynamic diameter and zeta potential were 19.6 wt.%, 36.7 ± 8.1 nm and -8.5 ± 1.3 mV, respectively. The 1-(4,5-dimethylthiazol-2-yl)-3,5-diphenyl-formazan (MTT) and 2′-deoxyguanosine 5′-monophosphate (d-GMP) was bought from Sigma–Aldrich. All the other reagents and solvents were purchased from Beijing Dingguo Changsheng Biotechnology Co. Ltd., China and used as received.

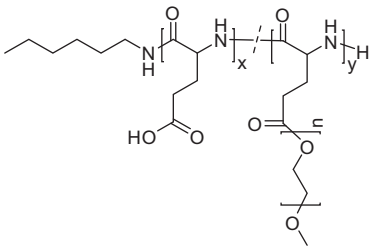

Scheme 1. Chemical structure of PLG-*g*-mPEG5K.

2.2. Characterizations

Gel permeation chromatography (GPC) measurements were conducted on a Waters GPC system (Waters Ultrahydrogel Linear column, 1515 HPLC pump with 2414 Refractive Index detector) using phosphate buffer (0.2 M, pH 7.4) as the eluent (flow rate: 1 ml/min, 25 °C, and polyethylene glycol as the standard). The particle sizes were measured by dynamic laser scattering (DLS) on a WyattQELS instrument with a vertically polarized He−Ne laser (DAWN EOS, Wyatt Technology). We measured the zeta-potentials with a Zeta Potential/BI-90Plus Particle Size Analyzer (Brookhaven, USA). Inductively coupled plasma mass spectrometry (ICP-MS, Xseries II, Thermoscientific, USA) was used for the quantitative determination of the levels of platinum. Matrix-assisted laser desorption/ionization time of flight mass spectrometry (MALDI-TOF-MS) measurements were carried out on a Bruker Autoflex III mass spectrometer operated in positive ion mode; the instrument was equipped with a 355 nm smartbeam laser. The accelerating voltage was maintained at 20 kV and 2,5-Dihydroxybenzoic acid was used as the matrix. We characterized the degradation products of PLG-*g*-mPEG5K using a MALDI-TOF-MS.

2.3. In vitro metabolism of PLG-g-mPEG5K

HeLa cells were seeded in 10 cm plates in 10 mL DMEM supplemented with 10% fetal bovine serum and incubated in a humidified 5% CO_2 atmosphere at 37 °C. When the plates were 50% confluent, the original medium was replaced with fresh serum-free DMEM that was supplemented with the PLG-*g*-mPEG5K copolymer at a final concentration of 500 μg/ml. The cells were incubated for 48, 96 or 144 h. The medium was collected and then extracted with dichloromethane (DCM). The organic phase was transferred to a clean tube and dried under nitrogen at room temperature. The extraction residue was measured by GPC and MALDI-TOF-MS. We incubated PLG-*g*-mPEG5K for 48, 96 or 144 h in cell culture medium without cells to be used as a negative control.

2.4. Influence of pH on the size of CDDP-NPs

CDDP-NPs were placed in a phosphate buffer (PB, 0.2 M) solution at a pH of 5.0, 6.0, 7.0 or 8.0. The hydrodynamic radius of the nanoparticles was measured with DLS.

2.5. Degradation of CDDP-NPs in aqueous solution

The degradation of CDDP-NPs in distilled water was evaluated at 4 and 37 °C in the dark. The concentrations used for this experiment were 0.5 mg/L on a CDDP basis. Each sample was placed in a glass vial wrapped in aluminum foil to prevent light exposure. We

used GPC to measure the average molecular weight and molecular weight distribution of each sample on day 0, 1, 2, 3, 14, 24 and 34.

2.6. Chelation with d-GMP

The CDDP-NPs (90.3 mg) were dispersed in 10 mL of a NaCl solution (0.9 wt.%) with the pH adjusted to 4.0 with 0.1 M HCl. Following a 2 day incubation at 37 °C with a shaking rate of 100 rpm, we transferred the solution (pH was changed to 4.6) into a dialysis tube (MWCO 500 Da) for 3 days to dialyze against deionized water (50 mL). We then collected the dialysate, added d-GMP (104.1 mg) and incubated the mixture at 37 °C with a shaking rate of 100 rpm. After 12 h, we collected the incubated solution for MALDI-TOF-MS analysis. For comparison, the CDDP (11.7 mg) was dissolved in deionized water (32.0 mL). Then d-GMP (67.4 mg) was added. The solution was incubated at 37 °C with a shaking rate of 100 rpm. After 12 h, we collected the incubated solution for MALDI-TOF-MS analysis.

2.7. In vitro cytotoxicity of CDDP-NPs

We assessed the *in vitro* cytotoxicity of CDDP-NPs using the MTT assay. LLC cells were seeded in 96-well culture plates at a density of 10^4 cells per well in 200 μL DMEM and allowed to adhere for 15 h. The culture medium was replaced with 200 μL of fresh medium containing free CDDP, PLG-*g*-mPEG5K or CDDP-NPs and allowed to incubate for an additional 48 h to 72 h. Then, 20 μL of MTT indicator dye (5 mg/mL in PBS, pH 7.4) was added to each well, and the cells were incubated for another 2 h at 37 °C in the dark. The absorbance of the solution was measured on a microplate reader (INFINITE 200 PRO, USA) at 490 nm. The relative cell viability was determined by comparing the absorbance of treated cells at 490 nm to control wells containing only cell culture medium. Data are presented as mean ± SD (n = 3).

2.8. Uptake of free CDDP and CDDP-NPs

LLC cells were seeded in 6-well plates at a density of 2.5×10^5 cells per well in 3.0 mL DMEM and incubated in a humidified 5% CO_2 atmosphere for 24 h. The original medium was replaced by fresh DMEM that was supplemented with CDDP (1.0 mg/L) or CDDP-NPs (1.0 mg CDDP equivalent/L). The cells were incubated for 1, 4, 12 or 24 h at 37 °C and then rinsed with cold PBS (1 mL × 3), and harvested with trypsin. The harvested cells were suspended in 1 mL of PBS and centrifuged at 1000 rpm for 5 min at 4 °C. The supernatants were discarded and the cell pellets were washed with 1 mL of PBS. After three cycles of washing and centrifugation, cells were re-suspended and diluted to a final volume of 1 ml in PBS. Cell numbers were counted, and then the cell suspensions were treated with nitric acid (68 vol.%) at 80 °C for 8 h. Platinum content was determined by ICP-MS analysis.

2.9. Hemolysis assay

We evaluated the hemolytic activity of PLG-*g*-mPEG5K, free CDDP and CDDP-NPs according to a reported protocol with slight modifications [23]. Briefly, fresh rabbit blood obtained from the Experimental Animal Center of the Jilin University was diluted using physiological saline. Red blood cells (RBCs) were then isolated from the serum by centrifugation. After careful washing, a suspension of RBCs was added into the PLG-*g*-mPEG5K, free CDDP or CDDP-NPs solution at systematically varied concentrations and mixed by vortexing. The mixture was kept in a 5% CO_2 atmosphere at 37 °C for 1.5 h. The samples were then centrifuged and transferred to 96-well plates. Free hemoglobin in the supernatant was measured with a Bio-Rad 680 microplate reader at 540 nm. The hemolysis ratio of RBCs was calculated using the following formula: Hemolysis (%) = $(A_{\text{sample}} - A_{\text{negative control}})/(A_{\text{positive control}} - A_{\text{negative control}}) \times 100$, where A_{sample}, $A_{\text{negative control}}$ and $A_{\text{positive control}}$ are the absorbance values of the samples, negative and positive controls. Physiological saline and distilled water were used as the negative and positive controls, respectively.

2.10. Animal use

Kunming mice (6–8 weeks old) were purchased from the Laboratory Animal Center, Jilin University, China. Male C_{57}BL/6 mice (6 weeks old, average body weight 22 g) were purchased from the Institute of Laboratory Animal Science of the Beijing Union Medical College, Chinese Academy of Medical Science, China. All the animals used in this paper were maintained under required conditions in accordance with evaluated guidelines and approved by the Animal Care Committee at the School of Public Health of the Jilin University.

2.11. Renal platinum accumulation

We administered free CDDP or the CDDP-NPs intravenously at a dose of 5 mg/kg on a CDDP basis to the Kunming mice (n = 3 per group). The mice were sacrificed at the defined time periods (10 min, 1 h, 6 h, 24 h, 48 h and 7 days). Both kidneys were excised and decomposed by heating in nitric acid. The platinum concentration in the solution was measured by ICP-MS.

2.12. In vivo antitumor efficacy of CDDP-NPs and survival rate

The Lewis lung carcinoma cells (2×10^5 cells) were inoculated subcutaneously into the right rear flank of each C_{57}BL/6 mouse. After the tumors reached about 100 mm^3, the mice were randomly divided into 5 groups containing 6 mice each. The mice were injected intravenously *via* a tail vein 5 times with saline, free CDDP (5 mg/kg), PLG-*g*-mPEG5K (100 mg/kg) or CDDP-NPs (5 mg/kg CDDP eq. or 10 mg/kg CDDP eq.) on days 1, 3, 5, 7 and 9. We evaluated the antitumor effect by measuring the tumor volume (V) according to the following equation: $V = a \times b^2/2$, where a and b were the major and minor axes of the tumors as measured by calipers, respectively. The body weight was measured simultaneously as an indicator of systemic toxicity. Moreover, the survival rates were monitored throughout the study.

3. Results and discussion

3.1. In vitro metabolism of PLG-g-mPEG5K

In order to evaluate the biodegradability of the PLG-*g*-mPEG5K copolymer, we measured metabolism *in vitro*. The PLG-*g*-mPEG5K copolymer was incubated in DMEM with or without HeLa cells and the intracellular degradation products were released into the cell culture medium. The degradation products were then extracted with DCM from the cell culture medium, collected and analyzed by GPC. As shown in Fig. 1, the DCM extraction residue exhibited a single peak at 16.6 min in the GPC spectrum following incubation with HeLa cells for 48 h. When we prolonged the time of incubation with the HeLa cells to 96 h, the GPC curve of the DCM extraction residues displayed two peaks at 17.3 min and 18.6 min. As the incubation time with HeLa cells was further increased to 144 h, the intensity of the peak at 17.3 min declined and the intensity of the peak at 18.6 min increased. These results indicate that the average molecular weight of the extraction residues declined as the incubation time with HeLa cells increased. In contrast, the DCM extraction residue at 48, 96 or 144 h taken from medium

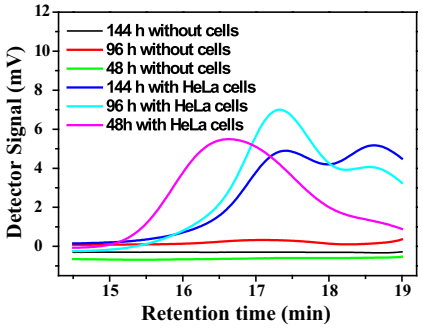

Fig. 1. GPC curves of the DCM extraction residues from incubation medium with or without HeLa cells in the presence of PLG-*g*-mPEG5K.

incubated without cells (negative control) did not show a peak in the GPC spectra (Fig. 1). It is important to note that the original PLG-*g*-mPEG5K copolymer is insoluble in DCM, whereas mPEG5K is highly soluble in DCM. Consequently, the DCM extraction residue from the incubation medium contains only degradation products with high mPEG5K content. Therefore, these GPC results suggest that the PLG-*g*-mPEG5K copolymer did not degrade in cell culture medium without cells, but was gradually degraded when incubated with the human HeLa cervical cancer cells.

To characterize the metabolic products following the *in vitro* metabolism of PLG-*g*-mPEG5K, the extraction residues at 144 h were analyzed by using MALDI-TOF-MS. As seen in Fig. 2, approximately 25 signals of fair abundance, all separated by 44 Da, appeared in the spectrum in the mass range 4400–5500 Da. These signals correspond to the formula of $CH_3O(CH_2CH_2O)_nGlu{\cdot}H^+$ (n = 97–121), indicating that the poly(glutamic acid) backbone of the PLG-*g*-mPEG5K polymer was degradable in the presence of the cells. A glutamic acid 5-mPEG ester [$CH_3O(CH_2CH_2O)_nGlu$] was generated in this process. Other metabolites of the PLG-*g*-mPEG5K polymer remain unknown.

3.2. Influence of pH on the size of CDDP-NPs

Because physiological pH values decrease from ~7.4 (blood) to ~6.8 (tumor-extracellular matrix) and ~5.0 (lysosome) along the endocytic pathway of nanoparticles [24,25], we investigated the influence of pH on the size of CDDP-NPs in an aqueous solution. Generally, pH has little influence on the size of CDDP-NPs. However, as shown in Fig. 3, the hydrodynamic radius (R_h) of the CDDP-NPs is 13.7 ± 1.0 nm at pH 5.0, 12.1 ± 0.9 nm at pH 6.0, 18.3 ± 0.8 nm at pH 7.0, and 16.6 ± 0.9 nm at pH 8.0, respectively. Therefore, the size of CDDP-NPs is slightly increased at higher pH values (pH 7.0 and 8.0). This may be due to increased deprotonation of free carboxy groups on the polymeric nanocarriers at high pH because the apparent pK_a of polyglutamic acid is closer to 6 [26].

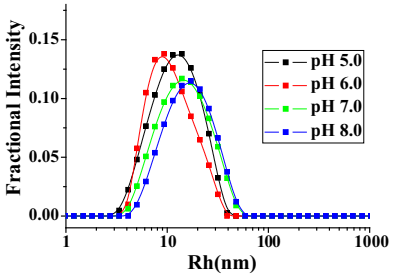

Fig. 3. Effect of pH on the hydrodynamic radius distribution of CDDP-NPs in an aqueous solution as determined by DLS.

Table 1
Degradation of CDDP-NPs in aqueous solution.

Days	4 °C		37 °C	
	$M_n \times 10^{-3}$ g/mol[a]	PDI[b]	$M_n \times 10^{-3}$ g/mol[a]	PDI[b]
0	35.2	1.57	35.2	1.57
1	32.4	1.66	31.6	1.65
2	37.1	1.57	33.3	1.52
3	34.0	1.69	31.7	1.53
14	35.2	1.68	24.1	1.40
24	38.4	1.69	29.2	1.29
34	35.6	1.60	19.6	1.10

[a] Number-average molar mass determined by GPC.
[b] Polydispersity index determined by GPC.

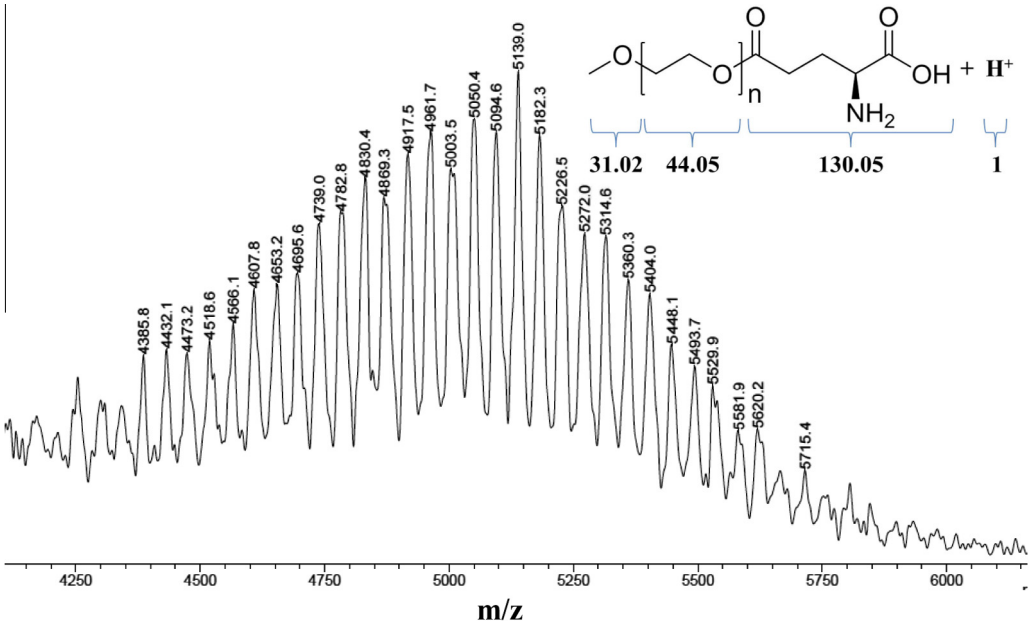

Fig. 2. MALDI-TOF-MS (range from m/z 4250 to 6000) of the DCM extraction residues from HeLa cell incubation medium in the presence of PLG-*g*-mPEG5K after a 144 h incubation period.

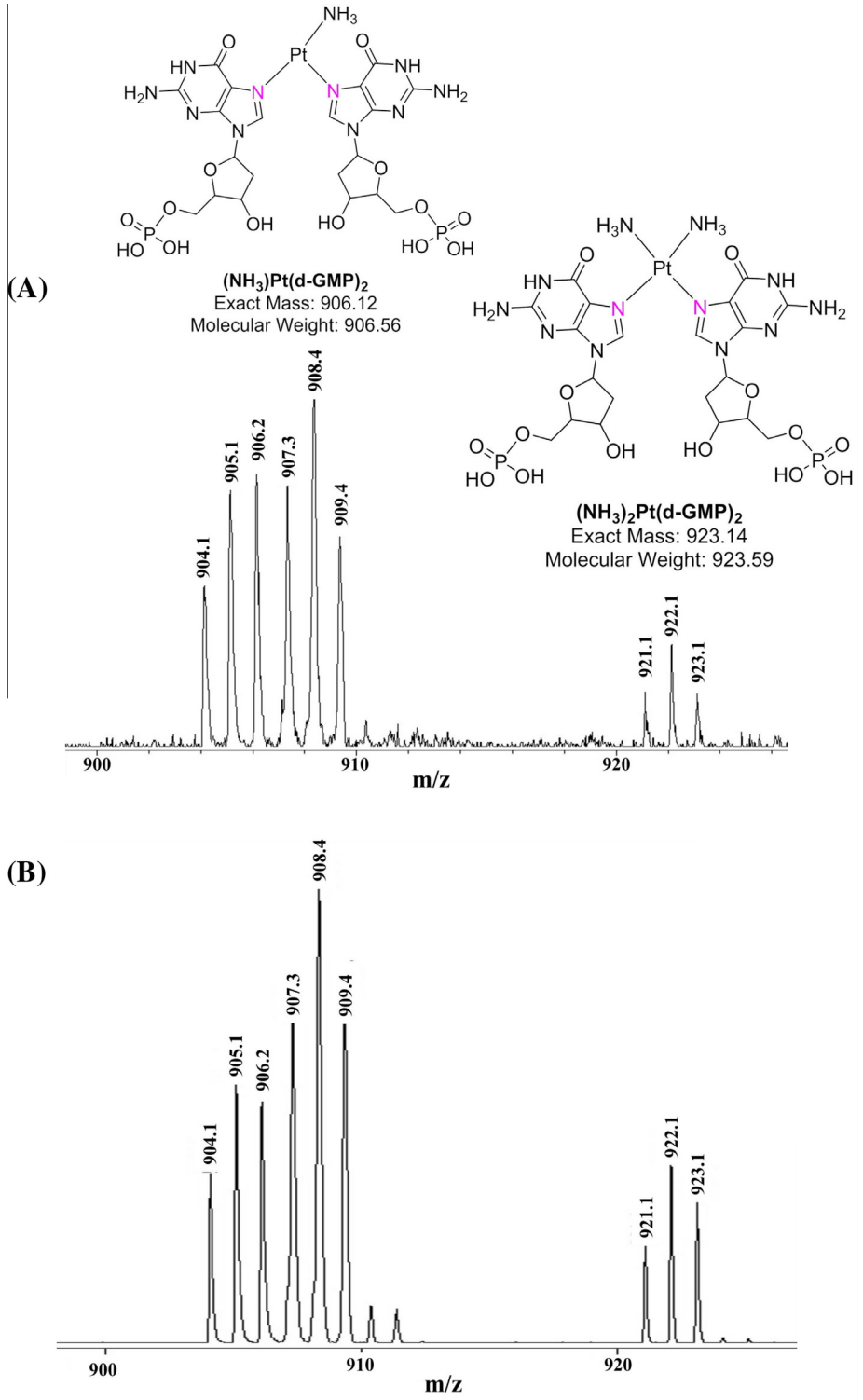

Fig. 4. MALDI-TOF-MS (range from $m/z = 900$ to $m/z = 950$). (A) Released Pt(II) species from the CDDP-NPs in the presence of d-GMP; (B) Pt(II) species from CDDP in the presence of d-GMP. The MS peaks at $m/z = 906.1$ and $m/z = 923.1$ correspond to the $[(NH_3)Pt(d\text{-}GMP)_2]$ and $[(NH_3)_2Pt(d\text{-}GMP)_2]$, respectively.

3.3. Degradation of CDDP-NPs in aqueous solution

The degradation of the CDDP-NPs was investigated in deionized water at 4 and 37 °C over a period of 34 days. As shown in Table 1, storage of CDDP-NPs in the aqueous solution at 4 °C revealed no significant degradation over the entire period. At a higher temperature (37 °C), the average molecular weight was decreased from an initial value of 35.2×10^3 g/mol to 19.6×10^3 g/mol at day 34. The gradual decrease of M_n is likely due to the hydrolysis of ester bonds and amide bonds on the PLG-*g*-mPEG5K copolymer of CDDP-NPs at higher temperatures in an aqueous solution.

3.4. Chelation with d-GMP

To evaluate whether CDDP-NPs would form cytotoxic DNA adducts, we analyzed the formation of Pt adducts using model

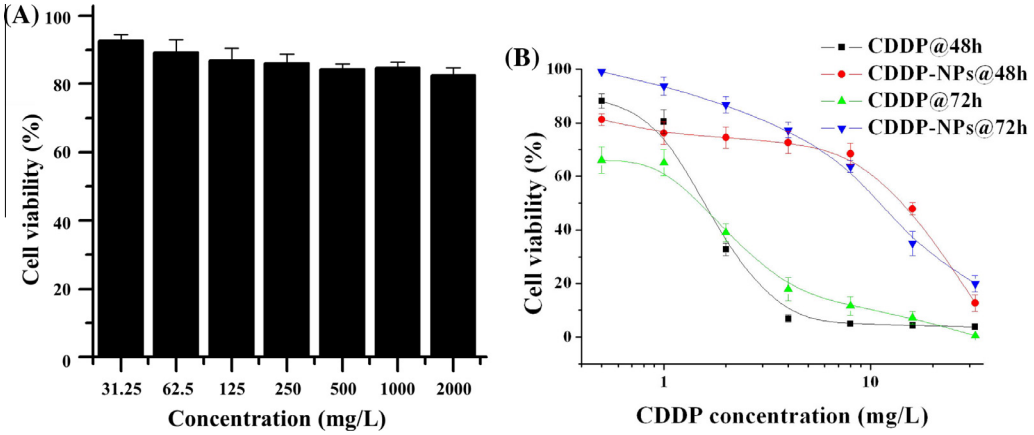

Fig. 5. *In vitro* cytotoxicity of PLG-*g*-mPEG5K copolymer, free CDDP, and CDDP-NPs to LLC cells. (A) PLG-*g*-mPEG5K copolymer incubated with LLC cells for 72 h; (B) CDDP and CDDP-NPs incubated with LLC cells for 48 and 72 h. The data are shown as mean ± SD ($n = 3$).

Table 2
The half maximal inhibitory concentration (IC_{50}) of free CDDP and the CDDP-NPs to the proliferation of LLC cells at 48 h and 72 h.

	IC_{50} at 48 h (mg/L)	IC_{50} at 72 h (mg/L)
Free CDDP	1.6	1.5
CDDP-NPs	14.4	11.1

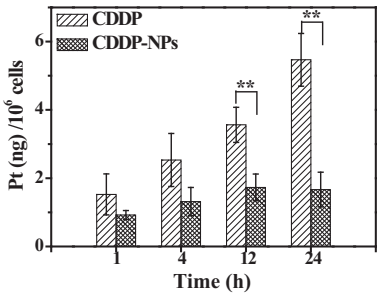

Fig. 6. LLC uptake of free CDDP (1.0 mg/L) and CDDP-NPs (1.0 mg CDDP equivalent/L). The data are shown as mean ± SD ($n = 3$), $^{**}p < 0.01$.

nucleotides of 2′-deoxyguanosine 5′-monophosphate (d-GMP) [27]. As shown in Fig. 4A, $[(NH_3)Pt(d\text{-}GMP)_2]$ and $[(NH_3)_2Pt(d\text{-}GMP)_2]$ were assigned to the MALDI-TOF-MS peaks corresponding to the released Pt(II) species from the CDDP-NPs in the presence of d-GMP at $m/z = 906.1$ and $m/z = 923.1$, respectively, indicating chelation with d-GMP. This suggests that release of active Pt(II) species from the CDDP-NPs chelate with d-GMP in the typical manner of a DNA crosslinking agent and implies that the CDDP-NPs would form cytotoxic DNA adducts and exert biological activity in a similar manner to cisplatin [28]. The Pt(II) species from CDDP in the presence of d-GMP exhibit a similar MALDI-TOF-MS spectrum (Fig. 4A) to the released Pt(II) species from the CDDP-NPs in the presence of d-GMP. This further confirms that CDDP from CDDP-NPs binds to DNA.

3.5. In vitro cytotoxicity and uptake assay

The relative cytotoxicity of the PLG-*g*-mPEG5K copolymer was assessed with MTT assays using an LLC cancer cell line. As seen in Fig. 5A, the viabilities of LLC cells treated with the PLG-*g*-mPEG5K copolymer were above 80% even at a concentration as high as 2.0 mg/mL, revealing that the PLG-*g*-mPEG5K copolymer had low toxicity and good cell compatibility.

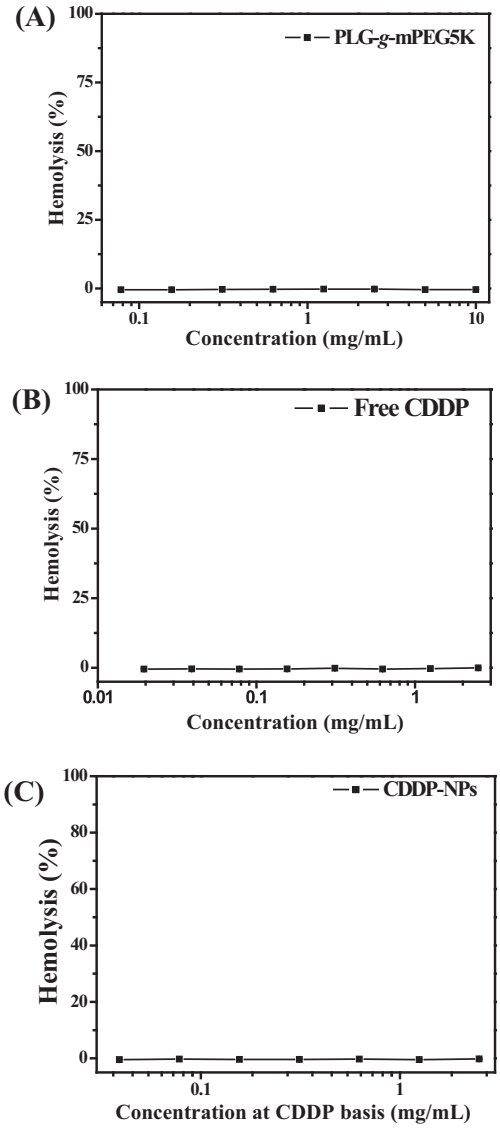

Fig. 7. Hemolysis assay (A) PLG-*g*-mPEG5K, (B) free CDDP and (C) CDDP-NPs.

To investigate the inhibition of the CDDP-NPs to LLC cancer cell proliferation *in vitro*, the cell viabilities were assessed after a 48 h or 72 h incubation period with the CDDP-NPs. Free CDDP was used

as the control. As shown in Fig. 5B and Table 2, both CDDP-NPs and free CDDP displayed obvious cytotoxicity to LLC cancer cells. CDDP-NPs showed dose and time dependent inhibition of LLC cell proliferation. The IC_{50} of CDDP-NPs to LLC cells at 48 h and 72 h was 14.4 and 11.1 mg/L, respectively. In contrast, free CDDP exhibited an IC_{50} of 1.6 and 1.5 mg/L at 48 h and 72 h, respectively. The *in vitro* cytotoxicity of CDDP-NPs to LLC cells was remarkably lower than that of free CDDP, which may be due, in part, to the slow release of CDDP from the CDDP-NPs. However, the relatively slower uptake of CDDP-NPs into the cells when compared to free CDDP is probably also responsible for the reduction in toxicity.

In order to examine the difference in cellular uptake between free CDDP and CDDP-NPs, LLC uptake experiments were carried out following a 1, 4, 12 or 24 h incubation period. As shown in Fig. 6, the cellular uptake of free CDDP was higher than that of the CDDP-NPs at 1 and 4 h. In particular, when the incubation time was extended to 12 or 24 h, the difference in cellular uptake between free CDDP and CDDP-NPs became significant. This may partially explain the reduction in toxicity to LLC cells treated with CDDP-NPs compared to free CDDP.

3.6. Hemolysis assay

Since the application of CDDP-NPs is based on intravenous injection, RBCs are the first cells they come in contact with after administration. Thus, hemolysis evaluation of the polymeric carriers and the CDDP-NPs is important. *In vitro* erythrocyte-induced hemolysis is a simple and reliable measure for estimating the hemocompatibility of materials. Furthermore, the behavior of the CDDP-NPs *in vivo* can be predicted by investigating the degree of hemolysis *in vitro* [29]. The hemolysis (%) represents the degree of RBC membranes destroyed by contact with various substances. A smaller rate of hemolysis indicates better blood compatibility. The hemolysis ratio of biomaterials must be below 5% for medical applications. The dose effects of PLG-*g*-mPEG5K copolymer, free CDDP, and CDDP-NPs on hemolysis are displayed in Fig. 7. The hemolysis ratio of the PLG-*g*-mPEG5K copolymer is close to zero even at a high concentration of 10.0 mg/L (Fig. 7A), indicating excellent hemocompatibility. Similar results were obtained for free CDDP (Fig. 7B) and the CDDP-NPs (Fig. 7C), suggesting that the PLG-*g*-mPEG5K and CDDP-NPs are hemocompatible and could be used for *in vivo* cancer treatment by intravenous administration.

3.7. Renal platinum accumulation

Since the main dose-limiting side effect of CDDP is nephrotoxicity, we investigated the renal platinum accumulation of the CDDP-NPs. As shown in Fig. 8, the mice treated with CDDP-NPs (5 mg/kg CDDP eq.) showed a remarkably lower peak renal platinum concentration (4.8×10^3 ng/g, 6 h) than mice treated with free CDDP (13.7×10^3 ng/g, 10 min). The kidney platinum level changed slowly from 4.4×10^3 ng/g at 10 min to 5.2×10^3 ng/g at 1 h after a single intravenous administration of the CDDP-NPs. In contrast, the platinum concentration in the kidneys decreased rapidly from 13.7×10^3 ng/g at 10 min to 8.3×10^3 ng/g at 1 h after the administration of free CDDP (5 mg/kg). These results indicate that administering CDDP-NP's results in a reduction of excreted platinum by the kidneys as compared to administering free CDDP at the same dosage. Since nephrotoxicity correlates with the peak urinary CDDP concentration [30], the CDDP-NPs have a decreased renal toxicity as compared to free CDDP [12,31].

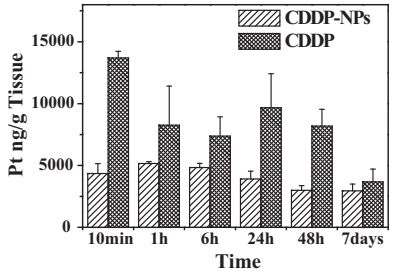

Fig. 8. Time course of kidney platinum accumulation from CDDP and CDDP-NPs in Kunming mice ($n = 3$, dosage: 5 mg/kg CDDP for CDDP, 5 mg/kg CDDP eq. for CDDP-NPs).

3.8. In vivo antitumor efficacy and survival rate

We used C_{57}BL/6 mice bearing LLC tumors to study the anticancer efficacy of CDDP-NPs. The mice were divided into 4 groups and injected 5 times at 2d intervals with saline, PLG-*g*-mPEG5K (100 mg/kg), free CDDP (5 mg/kg) and CDDP-NPs (5 mg/kg CDDP eq.) *via* the tail vein, respectively. Fig. 9A shows tumor growth curves after the first treatment. The PLG-*g*-mPEG5K copolymer did not suppress the LLC tumor growth. However, tumor growth was obviously inhibited in the groups injected with the CDDP-NPs or free CDDP. After 17 days, the tumor growth suppression rates due to treatment with the CDDP-NPs (5 mg/kg CDDP eq.), CDDP-NPs (10 mg/kg CDDP eq.) and free CDDP were 54.9%, 70.0% and 74.7%, respectively. Therefore, these data demonstrate that CDDP-NPs effectively prevented LLC tumor growth; though the

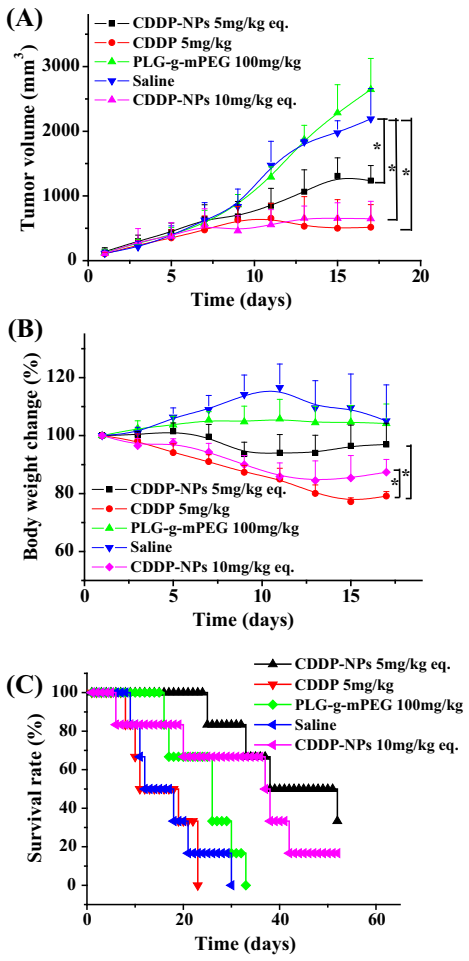

Fig. 9. Effect of CDDP formats on LLC tumor-bearing mice. (A) Tumor volume growth curve; (B) time course of changes in body weight; (C) time course of mouse survival rates. The mice were treated 5 times at 2-d intervals (Day 1, 3, 5, 7, 9). The data are shown as mean ± SD, $^*p < 0.05$.

effect of CDDP-NPs was less than free CDDP at the same dosage. Furthermore, suppression of the tumor growth rate increased with higher doses of CDDP-NPs. In fact, the CDDP-NPs exhibited comparable anticancer efficacy compared to free CDDP when the dosage was 2-fold higher.

Fig. 9B shows the loss in body weight in the LLC tumor-bearing mice 17 days following the first treatment. Body weights of the PLG-*g*-mPEG5K group were slightly increased, indicating that the polymer is non-toxic. After 17 days of treatment with CDDP-NPs, we observed increased losses in the percentage of body weight from 3.1% (5 mg/kg CDDP eq.) to 12.6% (10 mg/kg CDDP eq.), suggesting that the CDDP-NPs are toxic in a dose-dependent manner. In contrast, the average body weight loss of the free CDDP group was 20.8% at a dosage of 5 mg/kg CDDP. These results indicate that encapsulation of the PLG-*g*-mPEG5K copolymer reduces the systemic toxicity of free CDDP.

The survival rates of the LLC tumor-bearing mice are displayed in Fig. 9C. All mice treated with saline and the PLG-*g*-mPEG5K copolymer died within 33 days due to the highly aggressive nature of the murine Lewis lung cancer model [32,33]. In comparison, all animals died within 23 days after intravenous injection of free CDDP, owing to its severe toxicity. However, in the group of mice receiving the CDDP-NPs with 5 or 10 mg/kg CDDP eq., half survived for 37 days. In particular, of the mice receiving the CDDP-NPs (5 mg/kg CDDP eq.), 2 of 6 survived during the 52-day duration. The median survival times for the groups receiving saline, free CDDP (5 mg/kg), PLG-*g*-mPEG5K (100 mg/kg), CDDP-NPs (5 mg/kg CDDP eq.) and CDDP-NPs (10 mg/kg CDDP eq.) were 17, 18, 25, 51, and 37 days, respectively. These data suggest that the survival rates of tumor-bearing mice treated with CDDP-NPs are significantly higher than mice treated with free CDDP. This may be due to the acceptable antitumor efficacy and lower systemic toxicity of the cisplatin-loaded nanoparticles.

4. Conclusion

In this study, CDDP-loaded PLG-*g*-mPEG5K nanoparticles (CDDP-NPs) were characterized and exploited for the treatment of non-small cell lung carcinoma. We demonstrated that the poly(glutamic acid) backbone of the PLG-*g*-mPEG5K copolymer was cleaved *in vitro* to yield the glutamic acid 5-mPEG ester [$CH_3O(CH_2CH_2O)_n$Glu] in the presence of HeLa cells. The size of the CDDP-NPs could be slightly affected by varying the pH of the environment in the range of 5.0–8.0. In addition, the degradation of the CDDP-NPs in an aqueous solution was dependent on temperature. At a low temperature (4 °C), the CDDP-NPs were quite stable and, in general, the CDDP-NPs demonstrated a biological activity that is similar to cisplatin. Mice treated with CDDP-NPs showed a remarkably lower peak renal platinum concentration than mice treated with free CDDP at the same dosage, suggesting that renal toxicity is lower following treatment with CDDP-NPs compared to free CDDP. The PLG-*g*-mPEG5K copolymer and CDDP-NPs have excellent hemocompatibility. CDDP-NPs inhibited the proliferation of Lewis lung carcinoma cells *in vitro* and *in vivo*. Treatment with the CDDP-NPs improved the survival rates of tumor-bearing mice (median survival time: 51 days) compared to treatment with free CDDP (median survival time: 18 days), due to their acceptable antitumor efficacy and lower systemic toxicity. These results indicate that the CDDP-NPs have potential for the treatment of non-small cell lung carcinoma.

Acknowledgments

This research was financially supported by National Natural Science Foundation of China (Projects 51173184, 51373168, 51473029, 51233004 and 51390484), Ministry of Science and Technology of China (International Cooperation and Communication Program 2011DFR51090), and the Program of Scientific Development of Jilin Province (20130206066GX, 20130727050YY and 20130521011JH).

Appendix A. Figures with essential color discrimination

Certain figures in this article, particularly Figs. 1, 3–5 and 9 are difficult to interpret in black and white. The full color images can be found in the on-line version, at http://dx.doi.org/10.1016/j.actbio.2015.02.009.

References

[1] Siegel R, Ma J, Zou Z, Jemal A. Cancer statistics, 2014. CA Cancer J Clin 2014;64:9–29.
[2] Siegel R, DeSantis C, Virgo K, Stein K, Mariotto A, Smith T, et al. Cancer treatment and survivorship statistics, 2012. CA Cancer J Clin 2012;62:220–41.
[3] Beasley MB, Brambilla E, Travis WD. The 2004 World Health Organization classification of lung tumors. Semin Roentgenol 2005;40:90–7.
[4] Govindan R, Page N, Morgensztern D, Read W, Tierney R, Vlahiotis A, et al. Changing epidemiology of small-cell lung cancer in the united states over the last 30 years: analysis of the surveillance, epidemiologic, and end results database. J Clin Oncol 2006;24:4539–44.
[5] Pao W, Girard N. New driver mutations in non-small-cell lung cancer. Lancet Oncol 2011;12:175–80.
[6] Paramanathan A, Solomon B, Collins M, Franco M, Kofoed S, Francis H, et al. Patients treated with platinum-doublet chemotherapy for advanced non-small-cell lung cancer have inferior outcomes if previously treated with platinum-based chemoradiation. Clin Lung Cancer 2013;14:508–12.
[7] Goffin J, Lacchetti C, Ellis PM, Ung YC, Evans WK, Evidence CCOP. First-line systemic chemotherapy in the treatment of advanced non-small cell lung cancer a systematic review. J Thorac Oncol 2010;5:260–74.
[8] Jamieson ER, Lippard SJ. Structure, recognition, and processing of cisplatin-DNA adducts. Chem Rev 1999;99:2467–98.
[9] Zhou D, Xiao H, Meng F, Li X, Li Y, Jing X, et al. A polymer–(tandem drugs) conjugate for enhanced cancer treatment. Adv Healthc Mater 2013;2:822–7.
[10] Tanida S, Mizoshita T, Ozeki K, Tsukamoto H, Kamiya T, Kataoka H, et al. Mechanisms of cisplatin-induced apoptosis and of cisplatin sensitivity: potential of BIN1 to act as a potent predictor of cisplatin sensitivity in gastric cancer treatment. Int J Surg Oncol 2012;2012:8.
[11] Yao X, Panichpisal K, Kurtzman N, Nugent K. Cisplatin nephrotoxicity: a review. Am J Med Sci 2007;334:115–24.
[12] Uchino H, Matsumura Y, Negishi T, Koizumi F, Hayashi T, Honda T, et al. Cisplatin-incorporating polymeric micelles (NC-6004) can reduce nephrotoxicity and neurotoxicity of cisplatin in rats. Br J Cancer 2005;93:678–87.
[13] Beladi Mousavi SS, Hossainzadeh M, Khanzadeh A, Hayati F, Beladi Mousavi M, Zeraati AA, et al. Protective effect of forced hydration with isotonic saline, potassium chloride and magnesium sulfate on cisplatin nephrotoxicity: an initial evaluation. Asia Pac J Med Toxicol 2013;2:136–9.
[14] Morgan KP, Buie LW, Savage SW. The role of mannitol as a nephroprotectant in patients receiving cisplatin therapy. Ann Pharmacother 2012;46:276–81.
[15] Ghorbani A, Omidvar B, Parsi A. Protective effect of selenium on cisplatin induced nephrotoxicity: a double-blind controlled randomized clinical trial. J Nephropathol 2013;2:129–34.
[16] Kidera Y, Kawakami H, Sakiyama T, Okamoto K, Tanaka K, Takeda M, et al. Risk factors for cisplatin-induced nephrotoxicity and potential of magnesium supplementation for renal protection. PLoS One 2014;9:e101902.
[17] Cabral H, Kataoka K. Progress of drug-loaded polymeric micelles into clinical studies. J Control Release 2014;190:465–76.
[18] Soo Choi H, Liu W, Misra P, Tanaka E, Zimmer JP, Itty Ipe B, et al. Renal clearance of quantum dots. Nat Biotech 2007;25:1165–70.
[19] Dhar S, Gu FX, Langer R, Farokhzad OC, Lippard SJ. Targeted delivery of cisplatin to prostate cancer cells by aptamer functionalized Pt (IV) prodrug-PLGA-PEG nanoparticles. Proc Natl Acad Sci USA 2008;105:17356–61.
[20] Jokerst JV, Lobovkina T, Zare RN, Gambhir SS. Nanoparticle PEGylation for imaging and therapy. Nanomedicine 2011;6:715–28.
[21] Wang AZ, Langer R, Farokhzad OC. Nanoparticle delivery of cancer drugs. Annu Rev Med 2012;63:185–98.
[22] Yu H, Tang Z, Zhang D, Song W, Zhang Y, Yang Y, et al. Pharmacokinetics, biodistribution and in vivo efficacy of cisplatin loaded poly(L-glutamic acid)-g-methoxy poly(ethylene glycol) complex nanoparticles for tumor therapy. J Control Release 2014. http://dx.doi.org/10.1016/j.jconrel.2014.12.022.
[23] Ahmad Z, Tang Z, Shah A, Lv S, Zhang D, Zhang Y, et al. Cisplatin loaded methoxy poly (ethylene glycol)-block-poly (L-glutamic acid-co-L-phenylalanine) nanoparticles against human breast cancer cell. Macromol Biosci 2014;14:1337–45.
[24] Huang Y, Tang Z, Zhang X, Yu H, Sun H, Pang X, et al. PH-triggered charge-reversal polypeptide nanoparticles for cisplatin delivery: preparation and *in vitro* evaluation. Biomacromolecules 2013;14:2023–32.

[25] Li Y, Gao GH, Lee DS. Stimulus-sensitive polymeric nanoparticles and their applications as drug and gene carriers. Adv Healthc Mater 2013;2:388–417.
[26] Dibbern EM, Toublan FJ-J, Suslick KS. Formation and characterization of polyglutamate core−shell microspheres. J Am Chem Soc 2006;128:6540–1.
[27] Warnke U, Rappel C, Meier H, Kloft C, Galanski M, Hartinger CG, et al. Analysis of platinum adducts with DNA nucleotides and nucleosides by capillary electrophoresis coupled to ESI-MS: indications of guanosine 5′-monophosphate O6–N7 chelation. ChemBioChem 2004;5:1543–9.
[28] Xiao H, Noble GT, Stefanick JF, Qi R, Kiziltepe T, Jing X, et al. Photosensitive Pt(IV)–azide prodrug-loaded nanoparticles exhibit controlled drug release and enhanced efficacy in vivo. J Control Release 2014;173:11–7.
[29] Ren L, Huang X-L, Zhang B, Sun L-P, Zhang Q-Q, Tan M-C, et al. Cisplatin-loaded Au–Au2S nanoparticles for potential cancer therapy: cytotoxicity, *in vitro* carcinogenicity, and cellular uptake. J Biomed Mater Res A 2008;85A:787–96.
[30] Levi FA, Hrushesky WJM, Halberg F, Langevin TR, Haus E, Kennedy BJ. Lethal nephrotoxicity and hematologic toxicity of cis-diamminedichloroplatinum ameliorated by optimal circadian timing and hydration. Eur J Cancer Clin Oncol 1982;18:471–7.
[31] Mizumura Y, Matsumura Y, Hamaguchi T, Nishiyama N, Kataoka K, Kawaguchi T, et al. Cisplatin-incorporated polymeric micelles eliminate nephrotoxicity, while maintaining antitumor activity. Cancer Sci 2001;92:328–36.
[32] Teicher BA, Menon K, Alvarez E, Galbreath E, Shih C, Faul MM. Antiangiogenic and antitumor effects of a protein kinase Cβ inhibitor in murine lewis lung carcinoma and human Calu-6 non-small-cell lung carcinoma xenografts. Cancer Chemother Pharmacol 2001;48:473–80.
[33] Shuman Moss LA, Jensen-Taubman S, Rubinstein D, Viole G, Stetler-Stevenson WG. Dietary intake of a plant phospholipid/lipid conjugate reduces lung cancer growth and tumor angiogenesis. Carcinogenesis 2014;35:1556–63.